Direct Observation of Magnetic Anisotropy in an Individual Fe_4 Single-Molecule Magnet

E. Burzurí,[1,*] A. S. Zyazin,[1] A. Cornia,[2] and H. S. J. van der Zant[1]

[1]*Kavli Institute of Nanoscience, Delft University of Technology, P.O. Box 5046, 2600 GA Delft, The Netherlands*

[2]*Department of Chemistry and INSTM, University of Modena and Reggio Emilia, via G. Campi 183, I-41100 Modena, Italy*

(Received 14 May 2012; published 4 October 2012)

We study three-terminal charge transport through individual Fe_4 single-molecule magnets. Magnetic anisotropy of the single molecule is directly observed by introducing a spectroscopic technique based on measuring the position of the degeneracy point as a function of gate voltage and applied magnetic field. A nonlinear field-dependence is observed which changes by rotating the sample and is, thus, a direct proof of magnetic anisotropy. The sensitivity of this method allows us to observe small changes in the orientation and magnitude of the anisotropy in different charge states. We find that the easy axes in adjacent states are (almost) collinear.

DOI: 10.1103/PhysRevLett.109.147203 PACS numbers: 75.50.Xx, 73.23.Hk, 73.63.−b, 75.30.Gw

Molecular spintronics proposes a new route to information storage and processing based on the electrical addressing of magnetic states in individual molecules [1,2]. Magnetic molecules usually have long spin coherence and spin relaxation times [3] which are of crucial importance for information processing. In addition, versatility in synthesis allows us to produce a wide variety of molecular systems with almost tailor-made properties. Single-molecule magnets (SMMs) [4,5] are of particular interest for their magnetic anisotropy, which lifts spin degeneracy even at zero field and generates an energy barrier U that opposes spin reversal. Under favorable conditions, the molecular spin and magnetic anisotropy can be relatively large producing a sizeable hysteresis; each molecule behaves, therefore, as a nanomagnet. Addressing the magnetic states of single molecules remains, however, a challenging task, in spite of recent efforts [6–8].

Early attempts to measure the properties of individual SMMs focused on Mn_{12} clusters [9,10] and were followed by experiments on Fe_4 complexes [11,12]. Alternatively, $TbPc_2$ molecules were deposited on carbon nanotubes [13] and graphene layers [14] attached to metallic electrodes. In these systems, the conductance through the carbon structure serves as a probe of molecular magnetic properties. Spin flips were measured this way. However, no direct evidence of the magnetic anisotropy in the current flowing through a magnetic molecule has been reported yet. For this same reason, little is known [11,12] about the changes of magnetic anisotropy when the molecule is electrically charged.

In this Letter, we report on single-electron transport through a single Fe_4 molecule in a three-terminal geometry sketched in Fig. 1(a). We measured the anisotropy of an individual SMM in different charge states by measuring the position of the charge degeneracy point as a function of magnetic field. This *gate-voltage spectroscopy* should be contrasted to conventional transport spectroscopy as the gate voltage is the only control parameter. Moreover, the method does not rely on the detection of single-electron transport (SET) or cotunneling excitations as in Ref. [11] and it is, therefore, less sensitive to the coupling Γ between molecule and electrodes; its applicability is, thus, more general [15].

In our experiments, we used a SMM with a formula $[Fe_4(L)_2(dpm)_6] \cdot Et_2O$ where Hdpm is 2,2,6,6-tetramethyl-heptan-3,5-dione and H3L is the tripodal

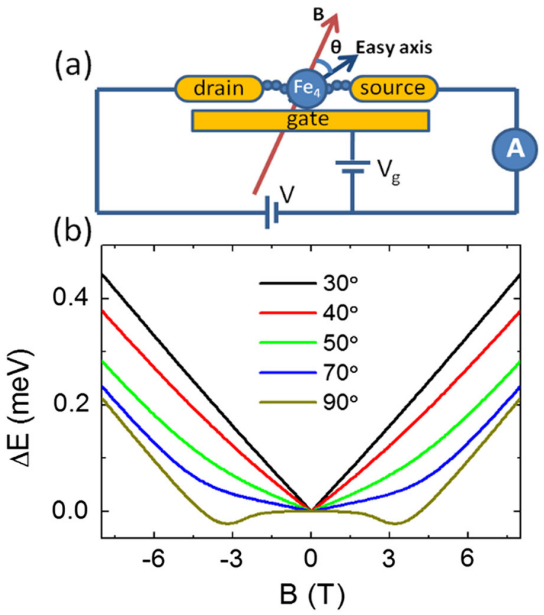

FIG. 1 (color online). (a) Schematic drawing of a Fe_4 single-molecule magnet in a three-terminal transistor geometry. A magnetic molecule bridges source and drain electrodes made by self-breaking electromigration of a gold nanowire. The gate electrode is used to access different redox states of the molecule. (b) ΔE vs B calculated by numerical diagonalization of Eq. (3) for different values of $\theta = \theta_N = \theta_{N+1}$. We assume $S_N = 5$ and $S_{N+1} = 9/2$. The anisotropy parameters are $D_N = D_{N+1} = 56\ \mu$eV as found in bulk samples. A nonlinear dependence of ΔE upon B can be observed for large values of θ, which is a fingerprint of magnetic anisotropy.

ligand 2-hydroxymethyl-2-phenylpropane-1,3-diol, which carries a phenyl ring [16] (see also the Supplemental Material [17]). The magnetic core is made of four Fe^{3+} ions ($s = 5/2$) coupled by antiferromagnetic exchange interactions to give a total molecular spin of $S = 5$ in the neutral state. The molecule presents a strong uniaxial anisotropy creating a preferential direction (easy axis) along which the molecular spin is aligned. Importantly, the stability of the Fe_4 molecules upon deposition on metallic surfaces has been demonstrated [18,19].

Nanometer-spaced electrodes were fabricated by self-breaking [20] of an electromigrated [21] gold nanowire immersed in a $10^{-4}M$ toluene solution of the molecules. Details on the transistor fabrication process are described elsewhere [12]. Three-terminal measurements were performed at a temperature $T \simeq 1.9$ K. The variation of the gate voltage allowed us to explore different charge states of Fe_4. Furthermore, to directly observe magnetic anisotropy, the angle between the easy axis and the applied magnetic field was changed. This change of orientation was realized by using a piezo-driven positioner that rotates the whole chip along an axis perpendicular to the magnetic field. The magnitude of the rotation (α) was determined by measuring the Hall voltage across a homemade Hall bar integrated into the chip carrier.

We measure 63 junctions of which six showed Coulomb blockade (see Supplemental Material [17]). In Fig. 2(a), we present the differential conductance (dI/dV) map as a function of the bias (V) and the gate (V_g) voltages at zero magnetic field for a particular junction. The plot shows lines of high-differential conductance characteristic of single-electron transport through the molecule. Low-differential conductance regions (Coulomb diamonds [22]) are visible in which the charge is stabilized within the Fe_4 molecule and therefore, the current is suppressed. Higher-order tunneling excitations within the Coulomb diamonds are visible at zero bias, which are indicative of Kondo correlations [22–25]. In Fig. 2(a), these are present in adjacent charge states indicating that at least one of the charge states has a high-spin ground state ($S \geq 1$) [12]. The coexistence of Coulomb blockade with higher-order tunneling processes shows that the sample is in the intermediate coupling regime with the electrodes. The molecule-electrode coupling Γ can be estimated from the full width at half maximum (FWHM) of the dI/dV peak at the Coulomb diamond edge. We find $\Gamma = 3$ meV, a value that is larger than the effective energy barrier of the neutral Fe_4 ($U = 1.4$ meV). Therefore, SET excitations associated with spin excited states within the $S = 5$ spin multiplet cannot be resolved.

The crossing point of the SET lines at zero bias, called the degeneracy point, fixes the ground state to ground state transition ($S_N \rightarrow S_{N+1}$) between adjacent charge states N and $N + 1$ with energies E_N and E_{N+1} [26]. The position of the peak in V_g depends on the energy difference

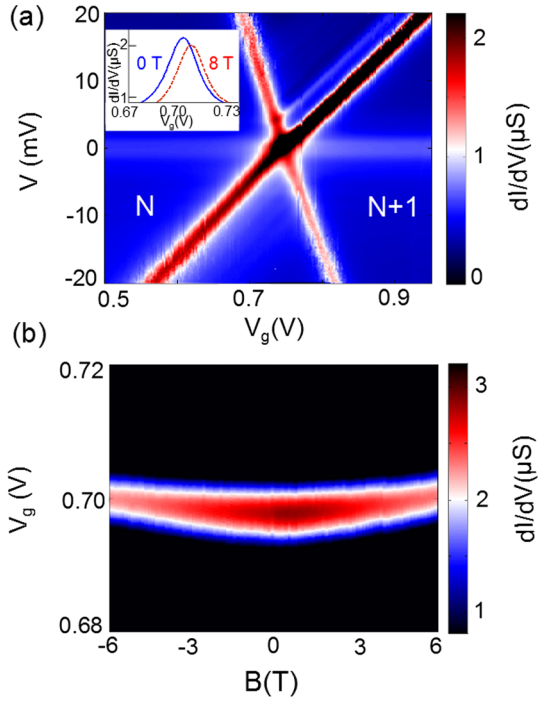

FIG. 2 (color online). (a) Color plot of dI/dV vs V and V_g at $T = 1.9$ K and zero field. Left and right-hand blue areas (denoted by N and $N + 1$ to the left and right of the cross) are low differential conductance regions in which the charge state is stabilized within the Fe_4. Red-dark lines (dark cross) define high-conductance regions in which single-electron transport takes place through the Fe_4. The crossing point at zero bias indicates the ground state to ground state transition between two charge states. The inset shows dI/dV curves as a function of V_g at zero bias measured at $B = 0$ and $B = 8$ T. (b) dI/dV color plot around the degeneracy point as a function of B and V_g measured at zero bias.

$E_{N+1} - E_N$ which can be tuned by applying a magnetic field. If the molecule is isotropic, such an energy difference varies linearly with the magnetic field B:

$$\Delta E(B) = [E_{N+1}(B) - E_N(B)] - [E_{N+1}(0) - E_N(0)] = -g\mu_B B \Delta S, \quad (1)$$

where $\Delta S = S_{N+1} - S_N$, g is the Landé factor and μ_B the Bohr magneton. This change of the chemical potential corresponds to a shift in the position of the dI/dV peak by

$$\Delta V_g(B) = \Delta E(B)/\beta = -g\mu_B B \Delta S/\beta, \quad (2)$$

where β is the gate coupling parameter [27]. Note that we have chosen $\Delta E(B = 0) = 0$ as Eq. (1) does not include terms independent of the magnetic field such as the electrostatic charging energy (energy needed to add or remove one electron). These terms determine the position of the peak at zero field but do not contribute to the shift in $V_g(B)$.

If the molecule is anisotropic, however, its spectrum depends on the mutual orientation of the magnetic field

and anisotropy axes, and the energy evolution $\Delta E(B)$ can, thus, be nonlinear. A simple model to describe the magnetic properties of an anisotropic SMM in the N-th charge state is the spin Hamiltonian:

$$H_N = -D_N S_{z,N}^2 + g\mu_B \vec{B} \cdot \vec{S}_N, \quad (3)$$

where the first term is the uniaxial magnetic anisotropy (chosen to be along the z axis), whose magnitude is denoted by the parameter D_N. The second term is the Zeeman interaction of the spin $\vec{S}$ with an external magnetic field $\vec{B}$. Importantly, the model predicts a nonlinear variation of the energy levels whenever the magnetic field is not collinear with z. Figure 1(b) shows $\Delta E(B)$ calculated by numerical diagonalization of the Hamiltonian of Eq. (3) for different angles θ between the easy axis and the magnetic field. We consider $D_N = D_{N+1} = 56\ \mu$eV (the bulk Fe_4 value [16]), $S_N = 5$, $S_{N+1} = 9/2$, and $\theta_N = \theta_{N+1} = \theta$. For high fields, ΔE is linear with the magnetic field for all values of θ since the Zeeman term dominates over the anisotropy term. The low-field behavior of ΔE is, in contrast, nonlinear for angles larger than 50° and the shape depends sensitively on the value of θ: magnetic anisotropy dominates over the Zeeman effect. The sign of the slope at high fields is determined by the difference in spin between adjacent charge states. According to Eq. (2), the slope is negative (positive) when $\Delta S > 0$ ($\Delta S < 0$) [28]. The plot, therefore, reveals whether the molecular spin increases or decreases upon reduction or oxidation of the molecule. The observation of a clear angular dependence as a function of B would, thus, be a direct evidence of the magnetic anisotropy of a single molecule addressed by an electric current.

The inset in Fig. 2(a) shows dI/dV as a function of V_g measured at two different magnetic field values (0 and 8 T) around the degeneracy point, i.e., it shows the zero-bias Coulomb peak. A lock-in modulation of 0.1 mV amplitude with no DC signal was applied between source and drain electrodes. A clear shift in the position of the peak maximum towards a higher gate voltage is observed. In order to better evaluate the evolution of ΔV_g with B, detailed measurements were carried out over the range $-6\ \text{T} \leq B \leq 6\ \text{T}$. The results are displayed in Fig. 2(b) as a dI/dV color plot as a function of B and V_g. The shape of the curve shows a nonlinear dependence with B indicating magnetic anisotropy.

For clarity, in Fig. 3, we show the position of the maxima extracted from Fig. 2(b), as a function of B (red open circles). The maxima are obtained by fitting the Coulomb peaks to Gaussian functions at each magnetic field. Peak voltages are then multiplied by the gate coupling $\beta = 0.08$ obtained from the slope [27] of the Coulomb diamonds in Fig. 2(a) so that the scale on the y-axis is in units of energy.

A direct proof of magnetic anisotropy was obtained by *in situ* rotation of the sample, i.e., by changing α. The measurement described in Fig. 2(b) was repeated after rotating the sample from α_1 to $\alpha_2 = \alpha_1 + 90°$. Figure 3

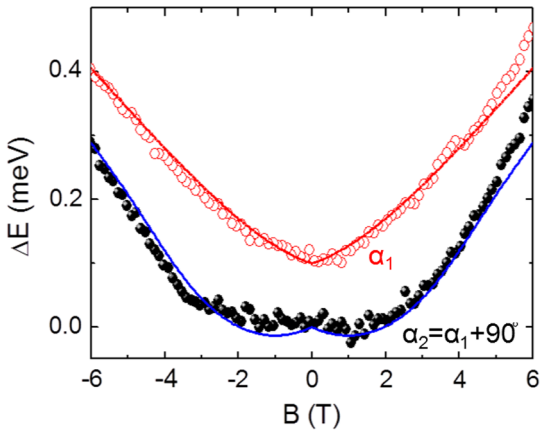

FIG. 3 (color online). Coulomb peak position as a function of B at two different angles α_1 and $\alpha_2 = \alpha_1 + 90°$. A vertical offset of 0.1 meV is introduced for clarity. The solid lines are calculations of ΔE by numerical diagonalization of the spin Hamiltonian in Eq. (3). Fitting parameters are: $S_N = 5$, $S_{N+1} = 9/2$, $D_N = 56\ \mu$eV, $D_{N+1} = 68\ \mu$eV. For α_1: $\theta_N = 63°$ and $\theta_{N+1} = 62°$. For α_2: $\theta_N = 87°$ and $\theta_{N+1} = 85°$. Other measurements at intermediate angles α are shown in the Supplemental Material [17].

compares the dI/dV peak positions for the two values of α (a vertical offset of 0.1 meV in ΔE was introduced for clarity). The low-field dependence differs significantly for these two angles, proving magnetic anisotropy unambiguously. The shape of the curves, according to Fig. 1(b), suggests a change to a larger value of θ when rotating to α_2.

To obtain a quantitative estimate of the anisotropy parameters, ΔE was analyzed using Eq. (3) and the results are given as solid lines in Fig. 3. In the calculation, we assumed that the g-factors are equal for both charge states ($g_N = g_{N+1} = 2$) and that the left-hand charge state is the neutral one ($S_N = 5$). Since ΔV_g is positive at high fields, the value of ΔS is negative according to Eq. (3) and therefore, the reduced spin state has $S_{N+1} = S_N - 1/2 = 9/2$ [29].

The anisotropy parameter D_N for the neutral state was assumed to be the bulk phase value ($D_N = 56\ \mu$eV) [16], as suggested by XAS measurements on molecules deposited on gold surfaces [18,19]. Free fitting parameters are then D_{N+1} and the two angles θ_N and θ_{N+1}. We found that the peak positions are well reproduced with $D_{N+1} = 68\ \mu$eV and the following angles: at α_1, $\theta_N = 63°$, and $\theta_{N+1} = 62°$; at α_2, $\theta_N = 87°$ and $\theta_{N+1} = 85°$. Note that θ changes by only 23° while rotating the sample by 90°. This suggests that the easy axis of the molecule and the rotation axis are closely aligned making the effective rotation smaller. The increase of the anisotropy parameter D when charging the molecule is consistent with our previous results [11].

The selection of the neutral charge state is arbitrary and an equally good fit could be obtained by assigning the right-hand charge state as the neutral one ($S_N = 5$).

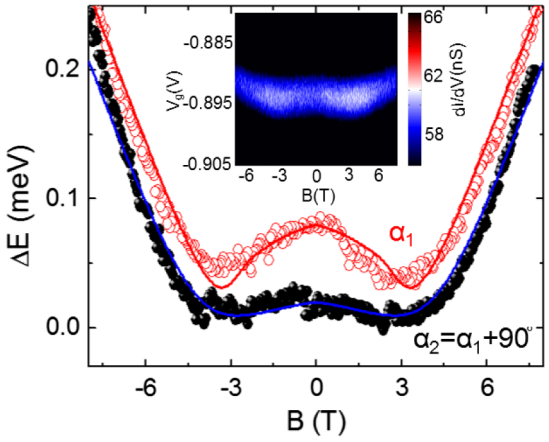

FIG. 4 (color online). Coulomb peak position as a function of B for a second sample of Fe_4 measured at two different angles α_1 and $\alpha_2 = \alpha_1 + 90°$. The solid lines are calculations of ΔE by numerical diagonalization of the spin Hamiltonian of the adjacent charge states. Fitting parameters are: $S_N = 5$, $S_{N+1} = 9/2$, $D_N = 56\ \mu$eV, and $D_{N+1} = 54.5\ \mu$eV. For α_1: $\theta_N = 90°$ and $\theta_{N+1} = 89.5°$. For α_2: $\theta_N = 82°$ and $\theta_{N+1} = 81°$. The inset shows the dI/dV color plot around the degeneracy point as a function of V_g and B at α_1.

According to Eq. (2), the oxidized spin state (left-hand) now has $S_{N-1} = 11/2$. Again, if we assume that the anisotropy in the neutral state is the same as in the bulk phase ($D_N = 56\ \mu$eV), the best fitting is obtained with $D_{N-1} = 47\ \mu$eV and the same angle values. In both scenarios, the qualitative conclusions are the same: upon reduction, the magnetic anisotropy increases and the spin state decreases.

The great sensitivity of the gate-voltage spectroscopy method can be used to study small changes of the magnetic anisotropy. In Fig. 4, we show the field dependence of dI/dV peaks measured for a second Fe_4 junction at two different angles α_1 and $\alpha_2 = \alpha_1 + 90°$ following the same method as described in Fig. 2. The slope of the curves at high fields is again positive meaning that S decreases upon reduction ($S_{N+1} < S_N$). The curve measured at α_1 shows a local maximum of about 0.05 meV around zero field that becomes less pronounced when the sample is rotated to α_2. The presence of a local maximum can be explained qualitatively: if θ_{N+1} is smaller than θ_N, the component of B parallel to the easy axis is larger for the $N+1$ state and therefore, at low fields, E_{N+1} changes faster than E_N and ΔE decreases. At high fields, the Zeeman contribution becomes dominant over the magnetic anisotropy and ΔE increases again. Solid lines shown in Fig. 4 are calculated by solving Eq. (3). Extensive analysis using Eq. (3) showed that the existence of a peak around $B = 0$ is only possible when θ_N is larger than θ_{N+1} and close to 90° (see Supplemental Material [17]). The magnitude of the maximum increases rapidly by increasing the difference $|\theta_{N+1} - \theta_N|$ in the model. Experimental data can be reproduced with misalignments of the easy axes of about 3°.

The presence and magnitude of a peak around $B = 0$, therefore, demonstrates that in adjacent states the easy axes are almost collinear.

The values obtained for D (see Fig. 4) are almost equal in the two charge states in contrast to the previous sample. However, it must be noticed that second order transverse anisotropy, not included in Eq. (3), may become relevant close to $\theta = 90°$. By introducing a transverse anisotropy term (E) of the order of the bulk value ($E = 2\ \mu$eV [16]), no significant change is, however, expected. Only by making E larger and of the order of $D/3$, sizeable changes can be observed when θ is close to 90° (see Supplemental Material [17]). In view of the large number of parameters, however, it is difficult to draw definite conclusions about the values of D and E when $\theta = 90°$. On the other hand, for $\theta = 90°$, gate-voltage spectroscopy may be a new tool to study and quantify quantum tunneling of the magnetization.

In summary, we have introduced gate-voltage spectroscopy as a transport spectroscopic technique to characterize individual magnetic molecules in different charge states. Using this method we directly observed the magnetic anisotropy in a single Fe_4 SMM and a decrease of the ground state spin upon reduction of the molecule. Moreover, the sensitivity of the technique revealed that the easy axes in adjacent charge states are only slightly misaligned ($\Delta\theta \sim 3°$).

This work was supported by FOM and the EU FP7 program under the Grant Agreement ELFOS.

*E.BurzuriLinares@tudelft.nl

[1] L. Bogani and W. Wernsdorfer, Nature Mater. **7**, 179 (2008).
[2] S. Sanvito, Chem. Soc. Rev. **40**, 3336 (2011).
[3] A. Ardavan, O. Rival, J. Morton, S. Blundell, A. Tyryshkin, G. Timco, and R. Winpenny, Phys. Rev. Lett. **98**, 057201 (2007).
[4] O. Kahn, *Molecular magnetism* (VCH Publishers, Inc., New York, 1993).
[5] D. Gatteschi, R. Sessoli, and J. Villain, *Molecular Nanomagnets* (Oxford University Press, Oxford, 2006).
[6] J. E. Grose, E. S. Tam, C. Timm, M. Scheloske, B. Ulgut, J. J. Parks, H. D. Abruña, W. Harneit, and D. C. Ralph, Nature Mater. **7**, 884 (2008).
[7] E. A. Osorio, K. Moth-Poulsen, H. S. J. van der Zant, J. Paaske, P. Hedegård, K. Flensberg, J. Bendix, and T. Bjørnholm, Nano Lett. **10**, 105 (2010).
[8] J. J. Parks *et al.*, Science **328**, 1370 (2010).
[9] H. B. Heersche, Z. de Groot, J. Folk, H. S. J. van der Zant, C. Romeike, M. Wegewijs, L. Zobbi, D. Barreca, E. Tondello, and A. Cornia, Phys. Rev. Lett. **96**, 206801 (2006).
[10] M. H. Jo, J. E. Grose, K. Baheti, M. M. Deshmukh, J. J. Sokol, E. M. Rumberger, D. N. Hendrickson, J. R. Long, H. Park, and D. C. Ralph, Nano Lett. **6**, 2014 (2006).
[11] A. S. Zyazin *et al.*, Nano Lett. **10**, 3307 (2010).

[12] A. S. Zyazin, H. S. J. van der Zant, M. R. Wegewijs, and A. Cornia, Synth. Met. **161**, 591 (2011).
[13] M. Urdampilleta, S. Klyatskaya, J.-P. Cleuziou, M. Ruben, and W. Wernsdorfer, Nature Mater. **10**, 502 (2011).
[14] A. Candini, S. Klyatskaya, M. Ruben, W. Wernsdorfer, and M. Affronte, Nano Lett. **11**, 2634 (2011).
[15] It also should be contrasted with the magneto-Coulomb effect in which transport takes place through a nonmagnetic molecule whose chemical potential is sensitive to the coupling with some external magnetic material. See, for instance: S. J. van der Molen, N. Tombros, and B. J. van Wees, Phys. Rev. B **73**, 220406 (2006); S. Datta, L. Marty, J. Cleuziou, C. Tilmaciu, B. Soula, E. Flahaut, and W. Wernsdorfer, Phys. Rev. Lett. **107**, 186804 (2011).
[16] S. Accorsi *et al.*, J. Am. Chem. Soc. **128**, 4742 (2006).
[17] See Supplemental Material at http://link.aps.org/supplemental/10.1103/PhysRevLett.109.147203 for more details about the Fe_4 SMM and statistics of the measurements. See also for details about the role of different D and θ in adjacent charge states and the transverse anisotropy parameter in the calculated ΔE.
[18] M. Mannini *et al.*, Nature Mater. **8**, 194 (2009).
[19] M. Mannini *et al.*, Nature (London) **468**, 417 (2010).
[20] K. O'Neill, E. A. Osorio, and H. S. J. van der Zant, Appl. Phys. Lett. **90**, 133109 (2007).
[21] H. Park, A. K. L. Lim, A. Paul Alivisatos, J. Park, and P. L. McEuen, Appl. Phys. Lett. **75**, 301 (1999).
[22] J. Park *et al.*, Nature (London) **417**, 722 (2002).
[23] D. Goldhaber-Gordon, D. Goldhaber-Gordon, H. Shtrikman, D. Mahalu, D. Abusch-Magder, and U. Meirav, Nature (London) **391**, 156 (1998).
[24] W. J. Liang, M. P. Shores, M. Bockrath, J. R. Long, and H. Park, Nature (London) **417**, 725 (2002).
[25] L. H. Yu and D. Natelson, Nano Lett. **4**, 79 (2004).
[26] Even if Γ is large, the ground state will be the most populated state and thus, we observe a peak at zerobias.
[27] E. A. Osorio, T. Bjørnholm, J.-M. Lehn, M. Ruben, and H. S. J. van der Zant, J. Phys. Condens. Matter **20**, 374121 (2008).
[28] Under the assumption that g is independent of the charge state.
[29] Spin blockade, seen as the suppression of SET at low bias, is not observed and we thus, assume $\Delta S = 1/2$.